

Role of uncrosslinked chains in the sliding dynamics of droplets on elastomers

Aurélien Hourlier-Fargette^{1,2}, Arnaud Antkowiak¹, Antoine Chateauminois³, and Sébastien Neukirch¹

¹ Sorbonne Universités, UPMC Univ Paris 06, CNRS, UMR 7190, Institut Jean Le Rond d'Alembert, F-75005 Paris, France

² Département de Physique, École Normale Supérieure, 24 rue Lhomond, F-75005 Paris, France.

³ ESPCI & CNRS, UMR 7615, Laboratoire de Sciences et Ingénierie de la Matière Molle, F-75005 Paris, France.

(Dated: November 30, 2016)

We observe and investigate an unexpected behavior in the dynamics of aqueous droplets sliding down on vertical plates of soft silicone elastomers, where two successive velocity regimes are present. This macroscopic observation is found to be closely related to microscopic phenomena at the scale of the polymer network: we demonstrate that uncrosslinked chains found in most widely used commercial elastomers are responsible for this surprising sliding behavior, and a direct visualization of these uncrosslinked oligomers is performed. The speed change is shown to be correlated to a sudden change of surface tension of the droplets.

Commonly used in the industry, silicone elastomers also serve as easy-to-make substrates in various research fields. Used in elastocapillarity, for both experiments on slender bendable structures [1, 2] and on thick softer substrates [3–6], they are even more widely spread in microfluidics, *e.g.* for biological cultures in microfluidic channels [7, 8]. However, drawbacks in the use of these polymers have been reported, for example absorption issues into the polymer bulk [9], or leaching of uncured oligomers from the polymer network into microchannel media [8]. Beyond the interest of understanding droplet dynamics on stiff inclined surfaces [10–15], the development of soft materials has lead to a growing interest for soft-wetting dynamics. A droplet deposited on a soft substrate is able to induce a wetting ridge at the contact line [5, 16], resulting in an additional source of dissipation when this triple line is moving [17]. Soft commercial elastomers like PDMS Sylgard 184 from Dow Corning are known to contain a small fraction of uncrosslinked low molecular-weight oligomers [18], the effects of which are not completely understood. Moreover, it has been shown recently that adhesion of a microbead on a soft elastomer gel leads to a phase separation which transforms the classical three-phase contact line into a four-phase contact zone, in which air, silica, liquid silicone, and silicone gel meet [19]. Here we show that uncrosslinked chains also play a major role in wetting dynamics in spite of their small proportion within the elastomers under consideration: A water-glycerol mixture droplet deposited on a vertical elastomer surface with no initial speed is shown to exhibit two different sliding regimes, as illustrated in Fig. 1 and in the Supplementary Video [20].

Unless otherwise specified, elastomer samples are made of poly(dimethylsiloxane) (PDMS, Sylgard 184 Elastomer base blended with its curing agent in proportion 10:1 by weight, cured during 2 hours at 60°C) molded in square Petri dishes to get flat samples with a thickness of a few millimeters. The Young's modulus of our PDMS samples was found to be $E = 1.8 \pm 0.1$ MPa. In order to prove the generality of the observed phe-

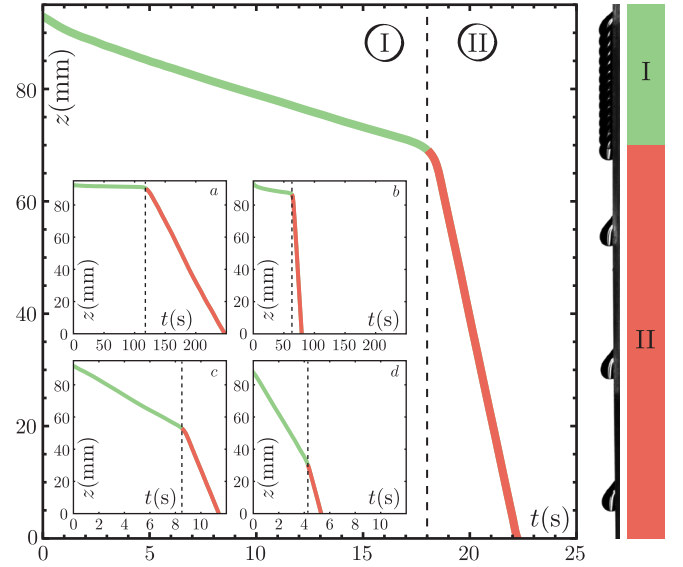


FIG. 1. A 40% water - 60% glycerol mixture droplet of volume $21.5\mu\text{L}$ is deposited with no initial speed on a vertical PDMS surface. Two regimes with two different constant speeds are identified (I and II). *Right*: Snapshots are taken every 1.28s and superimposed together. *Inset*: Same experiment with droplets of volumes $14\mu\text{L}$ (a), $18\mu\text{L}$ (b), $22.5\mu\text{L}$ (c) and $24\mu\text{L}$ (d).

nomenon, some experiments were also carried out using other commercial silicone elastomers, such as polyvinylsiloxane (PVS, Elite Double 22 Zhermack), RTV EC13 and EC33 polyaddition silicone polymer (Esprit Composite), and PDMS Sylgard 184 cured during 24h at 120°C. Droplets of water-glycerol mixtures (deionized water and glycerol 99+% pure, Acros Organics), which properties are given in Table I, are deposited on polymer samples with an electronic micropipette (Sartorius eLINE 5-120 μL). Videos have been captured with a Hamamatsu Orca Flash digital CMOS camera.

Fig. 1 shows the dynamics of a water-glycerol mixture droplet sliding down a vertical PDMS plate, showing

Gl.	Wa.	$T(^{\circ}\text{C})$	μ (mPa.s)	ρ (kg.m $^{-3}$)	γ (mN.m $^{-1}$)
50%	50%	19.3 ± 1.0	6.2 ± 0.2	1124 ± 1	69.0 ± 0.5
60%	40%	25.3 ± 1.0	8.7 ± 0.2	1150 ± 1	68.4 ± 0.5
65%	35%	27.0 ± 1.0	11.1 ± 0.2	1164 ± 1	67.9 ± 0.5
75%	25%	20.7 ± 1.0	34.1 ± 0.5	1192 ± 1	67.1 ± 0.5
85%	15%	27.5 ± 1.0	68.1 ± 1.0	1219 ± 1	66.5 ± 0.5

TABLE I. Mixing ratios (Gl. : glycerol, Wa. : deionized water), temperature T during the experiments, viscosity μ , density ρ and surface tension γ , measured for the different mixtures used.

two distinct sliding regimes with two different constant speeds. This two-regime behavior is observed for various droplet volumes (Inset of Fig. 1) and various water-glycerol mixing ratios, from pure water to 90% glycerol mixture. The same qualitative behavior is also obtained on several commercial silicone elastomers. This contrasts with experiments on treated glass [15] during which only one single speed is reached after a short transient.

Droplet dynamics on a vertical surface usually results from a competition between the weight of the droplet, capillary forces, and viscous dissipation inside the drop. For a droplet of volume V and density ρ on a vertical surface, the gravitational force is given by:

$$F_g = \rho V g. \quad (1)$$

The descent of the drop begins only if $F_g > F_{cl}$, F_{cl} being the contact line pinning force:

$$F_{cl} \propto \gamma w (\cos \theta_{sr} - \cos \theta_{sa}), \quad (2)$$

where γ is the surface tension of the liquid-air interface, w the width of the droplet, θ_{sr} the static receding angle and θ_{sa} the static advancing angle. A more precise determination of the onset of motion is given in [13]. Once steady motion is reached, the droplet speed is given by balancing its weight F_g with the sum of the contact line pinning force F_{cl} (written with the dynamic angles) and the viscous dissipation force in the droplet F_{μ} . F_{μ} can be derived using different approaches, depending on the dissipation being located in the bulk or in the receding corner of the droplet [21, 22]. The simplest approach gives:

$$F_{\mu} \propto \frac{\mu U S}{h}, \quad (3)$$

where U is the droplet speed, μ the viscosity of the liquid, S the contact area, and h the droplet height. For low Re viscous drops (with $Re = UV^{1/3}\rho/\mu$) this leads to a linear relationship between Ca and Bo where $Ca = \mu U/\gamma$ is the capillary number, and $Bo = \rho V^{2/3}g/\gamma$ is the Bond number. This description, as well as more detailed approaches taking into account the details of the viscous dissipation processes in the droplet [11, 12, 22] or in the

elastomer [3, 17, 23], cannot explain the two regimes in our experiments.

Different candidates can be responsible for the sudden change of the droplet speed: bistability, softness of the material, chemical interaction with the substrate, sliding to rolling transition, change of shape of the tail of the droplet and pearling transition [15, 24, 25]. Volumes have been kept under the threshold for which pearling occurs. Tracking particles in the water-glycerol mixture reveals that, in both regimes, the drop is rolling rather than sliding over the surface, with no significant difference in the motion of the fluid between the two regimes. Turning the setup upside down after a droplet has slid down allows us to reuse the same droplet and same sample for a second descent and to observe that the behavior of a droplet during the first descent is completely different from its behavior during the following descents. The first descent shows two distinct regimes, whereas the following descents only exhibit one regime, corresponding to the second regime of the first descent. This observation advocates for a chemical interaction with the substrate.

As explained in [18], when PDMS oligomers are crosslinked to form the polymer network, a few oligomer chains are not incorporated into the network. A PDMS sample thus contains uncrosslinked low-molecular-weight oligomers, which can be removed from the bulk PDMS by swelling in a good solvent. Treated PDMS samples were fabricated using the following procedure: The samples were placed for one week in a toluene bath, changed every day to prevent it from saturation in PDMS oligomers. During a second week, toluene was progressively replaced by ethanol, and the samples were then placed in a vacuum oven to evaporate all the solvents. An average mass loss of 5% was measured, corresponding to the removed uncrosslinked chains. A water-glycerol mixture droplet sliding down on such a treated elastomer only exhibits one sliding regime, as illustrated in Fig. 2. This one-regime behavior is observed for various droplet volumes and various water-glycerol mixing ratios, from pure water to 90% glycerol mixture. Reswelling this sample with a commercial PDMS v50 oil (Sigma Aldrich) enables us to recover the two-regimes behavior, as shown in the inset in Fig. 2. This experiment is a clear evidence of the crucial role played by the free oligomers of the substrate.

In the case of lubricant-infused surfaces, where a water drop rests on top of a thin layer of liquid oil, different wetting configurations are possible depending on the relative intensity of the surface tensions [26, 27]. Denoting γ_{wa} , γ_{wo} , and γ_{oa} the surface tensions of the water-air, water-oil, and oil-air interfaces respectively and introducing the wetting parameter $S = \gamma_{wa} - (\gamma_{wo} + \gamma_{oa})$, there are typically two possible situations for the wetting configuration: If $S > 0$ the oil completely covers the droplet and forms a thin film around it, whereas if $S < 0$ only a ridge of oil forms at the triple line. Now in the case where the substrate is a soft PDMS gel, uncrosslinked chains may

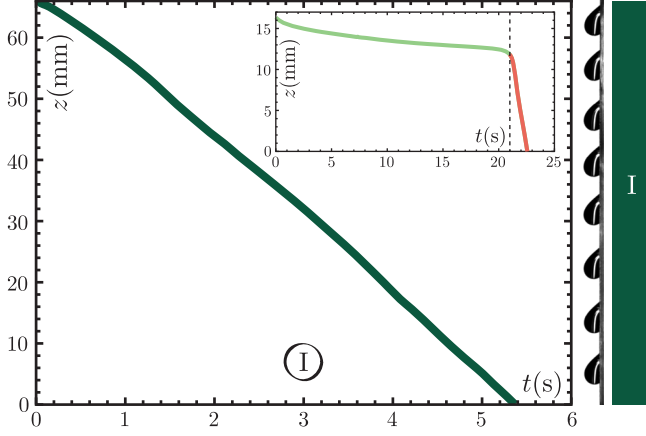


FIG. 2. A 40% water - 60% glycerol mixture droplet of volume $21.5\mu\text{L}$ is deposited with no initial speed on a vertical toluene-treated PDMS surface and a single regime is identified. *Right:* Snapshots are taken every 0.64s and superimposed together. *Inset:* Droplet dynamics on a toluene-treated PDMS sample re-swelled with commercial v50 PDMS oil. A 50% water - 50% glycerol mixture droplet of volume $18\mu\text{L}$ is deposited with no initial speed on a vertical surface and two different regimes with two constant speeds are identified.

phase-separate from the core of the gel and act as the thin layer of liquid oil mentioned above – such a phase separation was reported in the case of adhesion in [19]. Here we show that a water droplet can extract uncrosslinked oligomers from the PDMS elastomer, evidencing the existence of capillarity-induced phase separation at the triple line. Assuming that the uncrosslinked chains are quite similar to a commercial v50 PDMS oil [28], we find that such an oil has a positive spreading parameter on water and we conjecture the formation of a thin film of liquid PDMS around water droplets. This hypothetical oil film on a single droplet is anyhow invisible to the naked eye. However, collecting 1500 such droplets in a beaker after their two-regimes descent on an untreated PDMS sample results in a direct visualization of oil at the surface of the beaker, as shown on Fig. 3c. The control experiment on a toluene-treated PDMS sample leads to no visible oil at the surface of the beaker.

To further analyze the contribution of uncrosslinked chains to the droplet velocities, we focus on the surface tension of the droplets before sliding down and after reaching the second regime. An in-situ measurement of the droplet-air surface tension proves to be difficult, and hanging droplet measurements have the drawback of requiring droplet collection inside a capillary tube, possibly breaking a thin oil film present on the droplets. Thus, we designed the following setup: water-glycerol droplets of radius $r = 2.0$ mm are deposited thanks to a syringe pump onto an inclined PDMS plane (Fig. 3a). Droplets are sliding along the plane and collected in a 55mm diameter Petri dish after reaching the second regime. Surface

tension of the liquid in the Petri dish is then measured, using the ring method with a Krüss K6 manual tensiometer, as function of the collected volume both for droplets sliding down on untreated Sylgard 184 PDMS and on toluene-treated PDMS. For small volumes, the Petri dish is pre-filled with water, to allow for a measurement on a flat liquid-air interface. For the untreated sample, Fig. 3b shows a dramatic decrease of surface tension around a collected volume of 3 mL, which corresponds to about 100 droplets. If we assume that each droplet is covered by a homogeneous thin film of oil, the surface covered by this liquid oil in the Petri dish is about 100 times larger than on one single droplet. A collected volume of 3 mL thus corresponds to the situation for which the thickness of the oil film on the Petri dish is of the same order as the thickness of the oil film on a droplet in the second regime. We therefore conjecture that as the droplet is sliding down on PDMS it is gradually covered with oil and eventually submitted to a change of surface tension. Hence, we explain the sudden change in speed between the two regimes by a sudden change in surface tension. These results can be related to the surface tension measurements of a monolayer of PDMS oil spreading on water performed in [29].

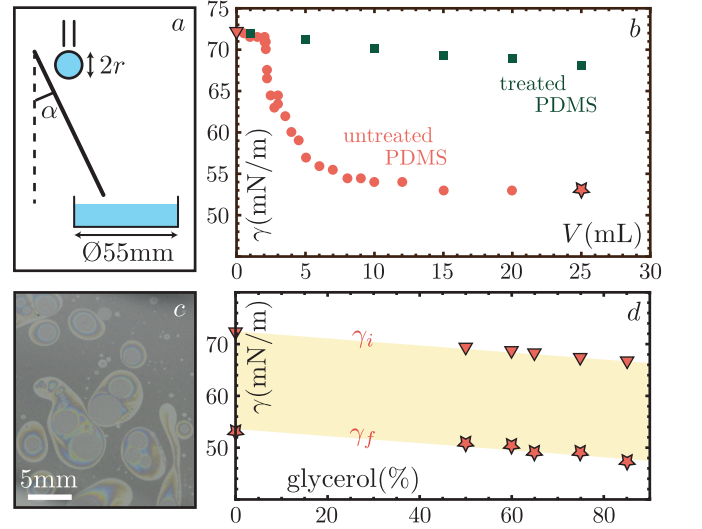


FIG. 3. (a) Experimental setup, with $\alpha = 29.2^\circ$ and $r = 2\text{mm}$. (b) Surface tension of given volumes of water droplets collected just after reaching the second sliding regime during their descent on untreated PDMS (red circles), compared to the same experiment performed on toluene-treated PDMS, with droplets collected after their descent on the 10cm sample (dark green squares). (c) Surface of a beaker in which 1500 water droplets (of $33\mu\text{L}$ each) were collected after reaching the second sliding regime. The colored zones correspond to thicknesses of the order of light wavelengths, and transparent lenses correspond to thicker oil zones. (d) Initial and final values of the surface tension for the different liquids described in Table I. Error bars are of the order of magnitude of the markers size.

The initial surface tension γ_i in the Petri dish before droplet collection, and the final surface tension γ_f measured when a 25mL volume of droplets has been collected are both shown on Fig. 3d as a function of water-glycerol mixing ratio. We see that the difference between the initial and final surface tensions is constant, $\gamma_i - \gamma_f \simeq 19$ mN/m.

A quantitative measurement of the velocities in the first and second regime on untreated PDMS, as a function of droplet volume is shown on Fig. 4a, for a 35% water and 65% glycerol mixture. The difference between the first and second regime speed is measured by looking at a vertical line drawn on this graph (black arrows). In the second regime, the surface tension of the droplet is lower than in the first regime, thus the pinning force is lower and the droplet goes faster. A slight change in contact angles is also observed.

A threshold volume can be defined for the first regime curve. This threshold divides the graph in two zones A and B. In zone A, the speed in first regime is zero, while the speed in the second regime has a finite value (even for small volumes, the speed in second regime has a low but finite value). In zone B, both speeds have a finite value. Examples for different water-glycerol mixing ratios are given on Fig. 4b and c. For a viscous fluid (Fig. 4c), the speed in the second regime is mostly determined by the fluid viscosity, whereas for a less viscous fluid (Fig. 4b), the viscosity of the uncrosslinked chains is shown to play an important role: The dissipation processes may be different in the first and second regimes.

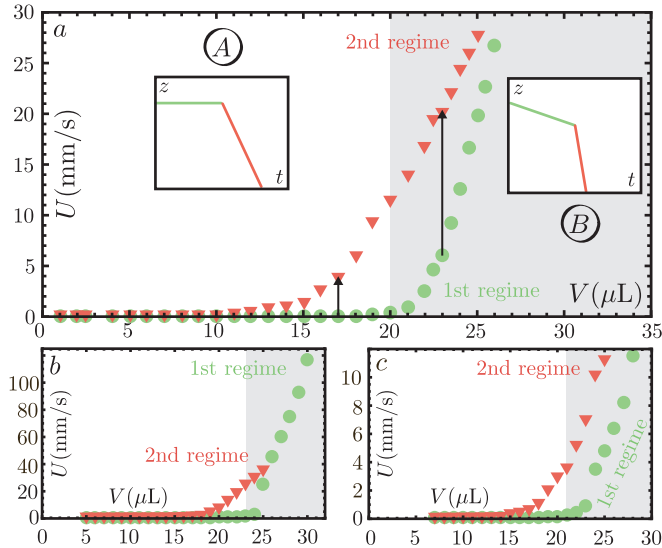


FIG. 4. (a) 65% glycerol - 35% water droplet speeds on untreated PDMS as a function of its volume, in first (light green circles) and second regime (red triangles). (b) Same experiment for a 50% glycerol - 50% water mixture. (c) Same experiment for a 85% glycerol - 15% water mixture. Error bars are of the order of magnitude of the markers size.

Fig. 5a compares the speeds measured in the first regime on untreated PDMS to the speeds measured on toluene-treated PDMS, for a 35% water and 65% glycerol mixture. The shape of these two curves is the same, except for the threshold volume value V_t below which the droplet speed is zero (Inset of Fig. 5a). The small difference in the threshold volumes V_t between the two curves can be explained by differences in advancing and receding angles on the two different samples. A droplet in the first regime on untreated PDMS behaves exactly as a droplet on a treated sample, i.e. as if it was not polluted by uncrosslinked oligomers. Fig. 5b and c proves the universality of this phenomenon by showing the collapse of all results of the experiments conducted with the different liquids mentioned in Table I, using the dimensionless numbers Ca and Bo .

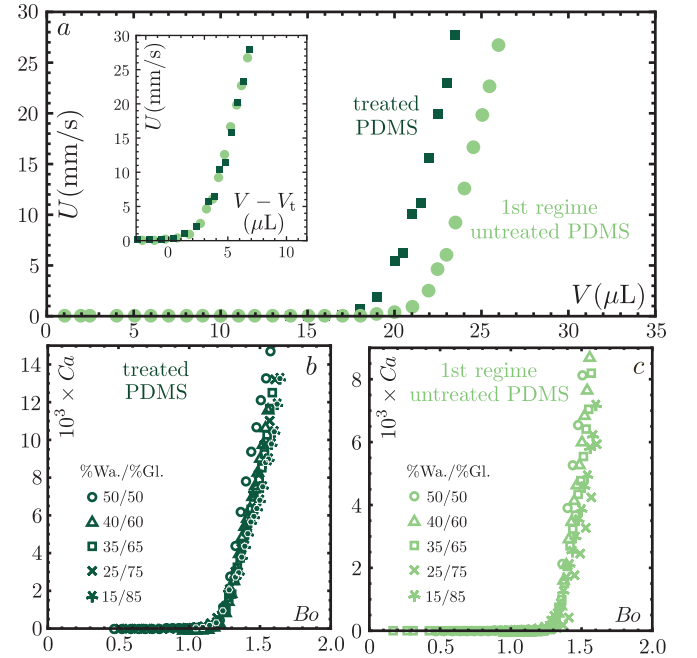


FIG. 5. (a) 65% glycerol - 35% water droplet speeds on treated PDMS (dark green squares) as a function of its volume, compared to the results for the first speed on untreated PDMS (light green circles). *Inset*: speeds as a function of the difference between the droplet volume V and the threshold volume V_t , on treated PDMS (dark green squares) and on untreated PDMS (light green circles). (b) and (c) Capillary number as a function of Bond number, for all liquids described in Table I. (b) corresponds to results on treated PDMS and (c) to results for the speed in the first regime on untreated PDMS. Error bars are of the order of magnitude of the markers size.

In summary, we have shown that uncrosslinked chains found in most commercial elastomers are responsible for an unexpected droplet sliding dynamics: an aqueous droplet deposited on a vertical elastomer plate exhibits successively two very different sliding regimes, with two different constant speeds. This phenomenon disappears

if the elastomer is treated in order to remove the uncrosslinked chains, and reappears when re-swelling such an elastomer with a silicone oil, thus demonstrating the crucial role of uncrosslinked chains in the droplet dynamics. Our study reveals how minute amounts of contaminants have dramatic effects on the wetting dynamics. A direct visualization of the oligomers has been performed at the surface of a liquid bath composed of thousands of droplets collected after their descent on untreated PDMS samples. We have also shown that the sudden in droplets velocities is linked to a sudden change of surface tension due to the surface contamination by silicone oligomers. Our findings could impact various research domains such as microfluidics or elastocapillarity as it contributes to a better knowledge of the interaction between water and silicon elastomers, and provides a simple test to evaluate the presence of unintended free oligomer chains by sliding water droplets on the sample surface.

We thank Laurent Limat, Cédric Boissière, Paul Grandgeorge, and Alexis Prevost for discussions. The present work was supported by ANR grant ANR-14-CE07-0023-01.

-
- [1] C. Py, P. Reverdy, L. Doppler, J. Bico, B. Roman, and C. N. Baroud, *Physical Review Letters* **98**, 156103 (2007).
 - [2] A. Fargette, S. Neukirch, and A. Antkowiak, *Phys. Rev. Lett.* **112**, 137802 (2014).
 - [3] A. Carré, J.-C. Gastel, and M. E. R. Shanahan, *Nature* **379**, 432 (1996).
 - [4] R. W. Style, C. Hyland, R. Boltyanskiy, J. S. Wettlaufer, and E. R. Dufresne, *Nat Commun* **4** (2013).
 - [5] S. J. Park, B. M. Weon, J. S. Lee, J. Lee, J. Kim, and J. H. Je, *Nat Commun* **5** (2014).
 - [6] S. Karpitschka, A. Pandey, L. A. Lubbers, J. H. Weijs, L. Botto, S. Das, B. Andreotti, and J. H. Snoeijer, *Proceedings of the National Academy of Sciences* **113**, 7403 (2016).
 - [7] E. Berthier, E. W. K. Young, and D. Beebe, *Lab Chip* **12**, 1224 (2012).
 - [8] K. J. Regehr, M. Domenech, J. T. Koepsel, K. C. Carver, S. J. Ellison-Zelski, W. L. Murphy, L. A. Schuler, E. T. Alarid, and D. J. Beebe, *Lab Chip* **9**, 2132 (2009).
 - [9] R. Mukhopadhyay, *Analytical Chemistry* **79**, 3248 (2007).
 - [10] C. Huh and L. Scriven, *Journal of Colloid and Interface Science* **35**, 85 (1971).
 - [11] O. V. Voinov, *Fluid Dynamics* **11**, 714 (1976).
 - [12] R. G. Cox, *Journal of Fluid Mechanics* **168**, 169 (1986).
 - [13] E. B. Dussan V., *Journal of Fluid Mechanics* **151**, 1 (1985).
 - [14] M. E. Shanahan and A. Carré, *Comptes Rendus de l'Académie des Sciences - Series IV - Physics* **1**, 263 (2000).
 - [15] N. Le Grand, A. Daerr, and L. Limat, *J. Fluid Mech.* **541**, 293 (2005).
 - [16] L. Limat, *The European Physical Journal E* **35**, 1 (2012).
 - [17] M. Shanahan and A. Carré, *Colloids and Surfaces A: Physicochemical and Engineering Aspects* **206**, 115 (2002).
 - [18] J. N. Lee, C. Park, and G. M. Whitesides, *Analytical Chemistry* **75**, 6544 (2003).
 - [19] K. E. Jensen, R. Sarfati, R. W. Style, R. Boltyanskiy, A. Chakrabarti, M. K. Chaudhury, and E. R. Dufresne, *Proceedings of the National Academy of Sciences* **112**, 14490 (2015).
 - [20] see Supplementary video SV1: 21.5 microliters droplet of 40% water 60% glycerol mixture sliding down on a vertical plate of PDMS (Sylgard 184 from Dow Corning), (2016).
 - [21] P.-G. de Gennes, F. Brochard-Wyart, and D. Quere, *Capillarity and Wetting Phenomena: Drops, Bubbles, Pearls, Waves* (Springer-Verlag New York, 2003).
 - [22] B. A. Puthenveetil, V. K. Senthilkumar, and E. J. Hopfinger, *Journal of Fluid Mechanics* **726**, 26 (2013).
 - [23] S. Karpitschka, S. Das, M. van Gorcum, H. Perrin, B. Andreotti, and J. H. Snoeijer, *Nat Commun* **6**, 7891 (2015).
 - [24] T. Podgorski, J.-M. Flesselles, and L. Limat, *Phys. Rev. Lett.* **87**, 036102 (2001).
 - [25] M. Ben Amar, L. J. Cummings, and Y. Pomeau, *Physics of Fluids* **15**, 2949 (2003).
 - [26] J. D. Smith, R. Dhiman, S. Anand, E. Reza-Garduno, R. E. Cohen, G. H. McKinley, and K. K. Varanasi, *Soft Matter* **9**, 1772 (2013).
 - [27] F. Schellenberger, J. Xie, N. Encinas, A. Hardy, M. Klapper, P. Papadopoulos, H.-J. Butt, and D. Vollmer, *Soft Matter* **11**, 7617 (2015).
 - [28] A more detailed description of the composition of uncrosslinked chains can be found in [8]: mass spectroscopy results give evidence of the presence of free chains of various lengths, in a continuous range of fewer than 20 to more than 90 dimethylsiloxane units.
 - [29] L. T. Lee, E. K. Mann, D. Langevin, and B. Farnoux, *Langmuir* **7**, 3076 (1991).